Sarthok Sircara, John G.Younger and David M. Bortz
Sticky surface: sphere - sphere adhesion dynamics
Journal of Biological Dynamics, 2015; 9(Suppl. 1):79-89

http://hdl.handle.net/2440/93832

Sticky surface: sphere–sphere adhesion dynamics

Sarthok Sircar[a], John G. Younger[b] & David M. Bortz[c]

[a] School of Mathematical Sciences, University of Adelaide,
Adelaide, SA 5000, Australia

[b] Department of Emergency Medicine, University of Michigan, Ann
Arbor, MI 48109 USA

[c] Department of Applied Mathematics, University of Colorado,
Boulder, CO 80309-0526 USA
Published online: 27 Aug 2014.

PLEASE SCROLL DOWN FOR ARTICLE

Taylor & Francis
Taylor & Francis Group

Sticky surface: sphere–sphere adhesion dynamics

Sarthok Sircar[a]*, John G. Younger[b] and David M. Bortz[c]

[a]School of Mathematical Sciences, University of Adelaide, Adelaide, SA 5000, Australia; [b]Department of Emergency Medicine, University of Michigan, Ann Arbor, MI 48109 USA; [c]Department of Applied Mathematics, University of Colorado, Boulder, CO 80309-0526 USA

We present a multi-scale model to study the attachment of spherical particles with a rigid core, coated with binding ligands and suspended in the surrounding, quiescent fluid medium. This class of fluid-immersed adhesion is widespread in many natural and engineering settings, particularly in microbial surface adhesion. Our theory highlights how the micro-scale binding kinetics of these ligands, as well as the attractive/repulsive surface potential in an ionic medium affects the eventual macro-scale size distribution of the particle aggregates (flocs). The bridge between the micro–macro model is made via an aggregation kernel. Results suggest that the presence of elastic ligands on the particle surface lead to the formation of larger floc aggregates via efficient inter-floc collisions (i.e. non-zero sticking probability, *g*). Strong electrolytic composition of the surrounding fluid favours large floc formation as well. The kernel for the Brownian diffusion for hard spheres is recovered in the limit of perfect binding effectiveness ($g \to 1$) and in a neutral solution with no dissolved salts.

Keywords: aggregation; sticking probability; binding ligands; Smoluchowski coagulation equations

1. Introduction

The formation of aggregates, induced by the adhesion of two spherical particles or nearby surfaces is important in many scientific and industrial processes. Interfacial attachment leading to larger floc aggregates via the latching of binders on surfaces in close proximity is widespread. Examples include binding of bacterial clusters to medical implants and host cell surfaces [39], cancer cell metastasis [22], and the coalescence of medical gels with nanoparticles for targeted drug delivery [25]. Moreover, coagulation and flocculation (the chemical and the physical aspects of adhesion) are also important in pulp and paper-making industries as well as waste water treatment plants [34]. This microscopic description of ligand-mediated surface adhesion is an important case from an experimental point of view, e.g. consider the experimental studies of the P-selectin/PSGL-1 catch bond interactions of leukocytes (a roughly spherical particle) with and without fluid flow [24,36]. The rigid microspheres in these case studies had much shorter bonds (no microvilli) and higher spring stiffness.

---

*Corresponding author. Email: sarthok.sircar@adelaide.edu.au

Author Emails: jyounger@med.umich.edu; dmbortz@colorado.edu

Past investigations in the micro-scale modelling of fluid-borne surface adhesion have addressed many theoretical challenges. These include the ligand-receptor binding kinetics [5,11], particle surface deformation [12,30], excluded volume effects [27], paramagnetism [29], short range interactions [38] and flow past the surrounding surfaces [14,20,37]. Consequently, many detailed kinetic models have successfully described the adhesion-fragmentation processes from the microscopic perspective. Korn and Schwarz [21] and more recently Mani *et al.* [23] studied the cellular adhesion between the ligand coated wall and a sphere moving in a shear flow. A similar model by Seifert *et al.* described the membrane adhesion via Langevin simulations [6]. On the contrary, the macro-scale phase-field models describe the geometry of the floc aggregates as a continuum mass of extracellular polymeric substance and predict the stability of the anisotropic structures in a flowing medium [9].

However, efforts to couple the microscopic ligand evolution kinetics of charged surfaces with the macroscopic population balance model, for particle aggregation dynamics, are limited. Sciortino *et al.* made a recent effort in this direction, but those numerical studies were done with chemically inert particles [10]. Other examples of recent work includes developing probabilistic extensions of Smoluchowski's multiplicative aggregation kernel in one [26] and two dimensions [19], with kernels containing one scaling parameter to be fit to data. Jia *et al.*, develop a method for predicting critical coagulant concentration via deriving a kernel incorporating surface charge density and potential as a function of the electrolyte [18]. Gilbert *et al.* investigated and validated the forces and potentials for nanoparticles [13] while Babler and Morbidelli studied aggregation and fragmentation, but only driven by diffusion and shear flow [3]. For a good overview of several research efforts as well as a focus on magnetic interactions, we direct the interested reader to Serrano *et al.* [31]. In summary, each of these research efforts have focused on the aggregation and fragmentation using separate theories.

This article represents an initial effort in providing a single unified theory by carefully coupling the micro-scale description of the overall aggregation rate with the macro-scale floc-size distribution. We explore how this adhesion (*collision* as termed in the colloid science literature) mechanism for rigid, micron-size, spherical flocs is governed by various geometric and fluid parameters as well as how the surface forces and binding kinetics of the ligands impact the eventual size of these flocs. Unlike results from our earlier paper [32], this work focuses on how to model the aggregation kernel, K_A, influenced by two microscopic effects (e.g. binding kinetics and surface charges). Furthermore, this modelling methodology gives an idea on how to extend other similar effects in future.

We consider the sphere–sphere interactions in a quiescent fluid conditions, thereby neglecting the effect of hydrodynamic interactions on the binders. This assumption is discussed in greater detail in Section 2.3. In the next section, we present the description of this population balance model, including the details of how to incorporate the effects of the micro-scale binder kinetics (Section 2.1), surface charges (Section 2.2) and finally, the model of the aggregation kernel (Section 2.3). In Section 3, we discuss the numerical results, including the surface potential and bond fraction calculations in Section 3.1 as well as the floc volume distribution dynamics in Section 3.2. We conclude with a brief discussion of the implication of these results and the focus of our future directions.

2. Mathematical model: binder kinetics, effect of surface charges and aggregation kernel

The present study is geared towards tracking the size distribution of spherical floc aggregates in stagnant fluid conditions [8]. The spherical particles within the flocs adhere through well-defined disc-like patches covered with binding ligands. Following the general outline given in [7], we define $b(t, x) \triangle x$, as the number of aggregates having volumes between x and $x + \triangle x$ in time t. In

the volumes between x_1 and x_2, the total number of flocs B_0 is given by

$$B_0(t, x_1, x_2) = \int_{x_1}^{x_2} b(t, x)\, dx \qquad (1)$$

for $[x_1, x_2] \subset [\underline{x}, \bar{x}]$, where $\underline{x}$ and $\bar{x}$ are the minimum and maximum aggregate volume sizes, respectively. The minimal size $\underline{x}$ is the volume of one particle, while $\bar{x}$ could go unrestrained (i.e. $\bar{x} \to \infty$). The conservation of the aggregate number density, or the Smoluchowski [33] coagulation equation for b is

$$b_t = A_{\text{in}}(x, b) - A_{\text{out}}(x, b), \qquad (2)$$

where A_{in} is the rate with which flocs of size in $[x, x + \triangle x]$ are created and A_{out} is the rate a floc of size in $[x, x + \triangle x]$ joins with another floc, to form a floc of volume greater than $x + \triangle x$. These rates are given by

$$A_{\text{in}}(x, b) = \frac{1}{2} \int_{\underline{x}}^{x - \underline{x}} K_A(y, x - y) b(t, y) b(t, x - y)\, dy, \quad x \in [2\underline{x}, \bar{x}], \qquad (3a)$$

$$A_{\text{out}}(x, b) = b(t, x) \int_{\underline{x}}^{\bar{x} - x} K_A(x, y) b(t, y)\, dy, \quad x \in [\underline{x}, \bar{x} - \underline{x}], \qquad (3b)$$

K_A is the aggregation kernel, describing the rate with which flocs of volume x and y combine to form a floc of volume $x + y$. The next three sections will focus on modelling this kernel based on (a) the surface binding kinetics and (b) surface potential, of two coalescing, charged spherical floc-surfaces.

2.1. *Surface binding kinetics*

Figure 1 illustrates a model of interfacial attachment between two spheres of radius R_1 and R_2 [11]. The centre, O, of the local spatial frame is located at the point of minimum separation and on the surface of sphere 2. The surface of the spheres bind onto each other due to the presence of adherent elastic binders (which are polymer strands with sticky heads) attached on the floc-surfaces. The floc core does not deform. The binders are idealized as linear Hookean springs with stiffness κ_0. The mean rest length (i.e. the uncompressed or the unstretched length) of the binders is l_0. For a given spatial point $\mathbf{s} = (s_1, s_2, s_3)$ with respect to the centre, O, of the local frame, let $D(\mathbf{s})$ be the separation distance between the two spheres, A_{Tot} and g be the total number and the fraction of effective binding ligands on the adhesion surface, respectively. For notational simplicity, we denote $D(\mathbf{s}) = D^*$. In the local frame, this separation distance is
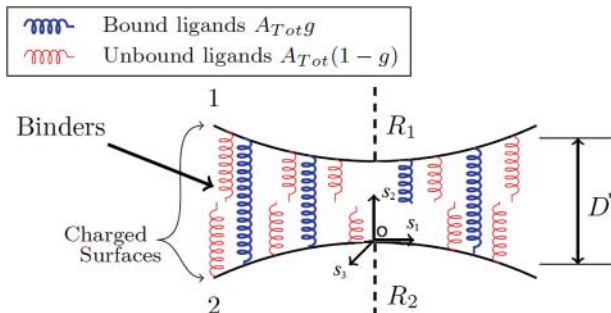
Figure 1. Closeup of the surface of two coalescing spherical, rigid flocs coated with binding ligands.

given by, $D^* = (s_1^2 + s_3^2)/2(1/R_1 + 1/R_2) + D$, where D is the minimum separation distance (Figure 1). Next, we define $A_{\text{Tot}}g(t)\,\mathrm{d}A$ as the number of bonds in the transverse direction that is attached between the two surfaces inside the circular patch, $\mathrm{d}A$, at time t. In colloid literature, the function g is synonymous to the term *sticking probability*. Hence the total number of bonds formed in the transverse direction is $\int_{A_s} A_{\text{Tot}}g(t)\,\mathrm{d}A$, A_s being the area of adhesion [11]. The bond attachment/detachment rates, are

$$K_{\text{on}}(D) = K_{\text{on,eq}} \exp\left[\frac{-\kappa_s(D - l_0)^2 + W(D)}{2k_BT}\right],$$

$$K_{\text{off}}(D) = K_{\text{off,eq}} \exp\left[\frac{(\kappa_0 - \kappa_s)(D - l_0)^2 + W(D)}{2k_BT}\right], \tag{4}$$

respectively, where $K_{\text{on,eq}}$ and $K_{\text{off,eq}}$ are the forward and reverse reaction rates for an undisturbed bond, k_B is the Boltzmann constant, T is the temperature, κ_s is the spring constant of the transition state used to distinguish catch ($\kappa < \kappa_s$) from slip ($\kappa > \kappa_s$) bonds [11], and $W(D)$ is the total surface potential (described in the next section). In the limit of small binding affinity ($K_{\text{eq}} = A_{\text{Tot}}K_{\text{on, eq}}/K_{\text{off, eq}} \ll 1$) and assuming that the binding ligands are abundant on the sphere surface [11], the evolution equation for g is therefore

$$\frac{\mathrm{d}g}{\mathrm{d}t} = A_{\text{Tot}}K_{\text{on}} - K_{\text{off}}g. \tag{5}$$

2.2. *Effect of surface charges*

We describe these interactions on the rigid surface of charged spherical flocs, through the Derjaguin, Landau, Verwey and Overbeek (DLVO) approach, i.e. the Coulombic and Van der Waals interaction. For simplicity we neglect non-DLVO interactions (e.g. steric repulsion, polymer bridging, hydration effects, and hydrophobic attraction) in this study. The potential due to the repulsive Coulombic forces is given by

$$W_C(D) = 2\pi\epsilon_0\epsilon\psi_1\psi_2\left(\frac{2R_1R_2}{R_1 + R_2}\right)\mathrm{e}^{-\kappa D}, \tag{6}$$

where R_1, R_2 are the radii of the charged spheres, D the minimum separation distance, κ the Debye length, ϵ, ϵ_0 the dielectric constant of vacuum and the medium, respectively and ψ_1, ψ_2 the *zeta potentials* of the respective spheres. The corresponding potential due to the attractive Van der Waal forces is

$$W_{\text{VW}}(D) = -\frac{A}{6D}\frac{R_1R_2}{R_1 + R_2}, \tag{7}$$

where A is the Hamaker constant, measuring the Van der Waal 'two-body' pair-interaction for macroscopic objects. The net surface potential is $W(D) = W_C(D) + W_{\text{VW}}(D)$, which is pair-wise attractive over very short and very long distances, and pair-wise repulsive over intermediate distances (Figure 2).

2.3. *Aggregation kernel*

First, we discuss some limitations imposed in our current approach. Due to stagnant fluid conditions, we neglect the shearing effect of the fluid flow on the mean rest length of the binders and the spatial inhomogeneities in the material parameters. This assumption allows us to study the attachment/detachment of the binders normal to the adhering surface (thereby ignoring
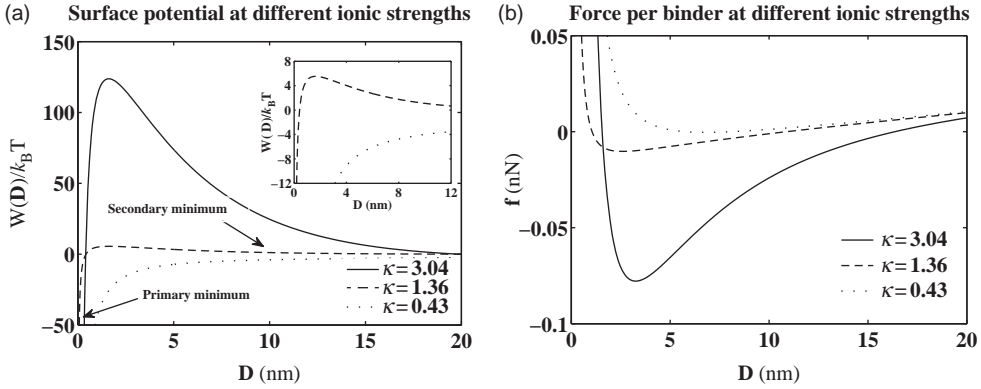
Figure 2. (a) Total surface potential, $W(D)$ versus the separation distance D, for two rigid, spherical flocs of radii $R_1 = 0.25\,\mu$m and $R_2 = 0.5\,\mu$m, respectively, and (b) surface force per binder, $\mathbf{f}$, (Equation (11)) versus D; at different ionic concentration of a 1:1 electrolyte. Regions of attraction: $\mathbf{f} > 0$, region of repulsion: $\mathbf{f} < 0$. The units of $\mathbf{f}$ are in nN.

the tangential displacement of the spheres) [32]. Furthermore, the binder kinetics is assumed to be independent of the salt concentration (i.e. the spring stiffness, κ_0 is independent of the charge-screening length, κ, and the zeta potentials, ψ_i. This implies that we are neglecting the electro-viscous stresses [35]). Compared with the time scale of floc aggregation (or the time scale on which the aggregate number density changes), the attachment/detachment rates of the flocs are sufficiently rapid so that the non-equilibrium binding kinetics can be ignored (i.e. $dg/dt = 0$ in Equation (5)). In this last assumption, we have ignored the anisotropic arrangement (or the fractal nature) of the flocs, i.e. the aggregation is followed by a quick restructuring step with very short relaxation time. Although this assumption may not be realistic in experiments but some groups have shown that the results are, otherwise, qualitatively similar [30]. We anticipate that the length-scales will be $\mathcal{O}(l_0)$, and hence introduce dimensionless variables. From now on we will denote the non-dimensional quantities with a superscript ($'$),

$$D = l_0 D', \quad t = t_0 t', \quad K_{\text{on/off}} = K_{\text{on/off,eq}} K'_{\text{on/off}}, \quad g = K_{\text{eq}} g', \tag{8}$$

where $t_0 = 1$ min represents the timescale of the duration of the experiments. Furthermore, we introduce the following non-dimensional parameters:

$$r = \frac{\kappa_0 l_0^2}{2 k_B T}, \quad \kappa'_s = \frac{\kappa_s}{\kappa_0}. \tag{9}$$

The non-dimensional form of the expression for the reaction rates (Equation (4)) and the fraction of effective ligands (after setting $dg/dt = 0$ in Equation (5)) respectively, reduce into

$$K'_{\text{on}} = \exp[-\kappa'_s r(D' - 1)^2 + W'(D)],$$
$$K'_{\text{off}} = \exp[(1 - \kappa'_s) r(D' - 1)^2 + W'(D)],$$
$$g' = e^{-r(D'-1)^2}. \tag{10}$$

We remark that $g' \in [0, 1]$ and the corresponding dimensional value of $g \in [0, K_{\text{eq}}]$. In the limit of small binding affinity ($K_{\text{eq}} \ll 1$), this value of g cannot exceed 1.

Under the influence of the binding kinetics and the surface charges, the instantaneous force due to one bound ligand is

$$\mathbf{f}'(D) = (D' - 1) + \nabla_D \cdot W'(D), \tag{11}$$

where $\mathbf{f}' = \mathbf{f}/f_0$ and $f_0 = \kappa_0 l_0$. The first term in Equation (11) represents the stretching force from the binder due to Hooke's law and the second term represents the force due to the surface potential. The direction of this force is along the normal to the two colliding surfaces, and along the direction vector from the spherical floc of radius R_2 towards the floc of radius R_1 (Figure 1). The total force arising from all such bound bonds on the floc surface, is therefore

$$\mathbf{F}'_{\text{Tot}}(D, t) = \int_{A'_s} A_{\text{Tot}} g'(t) \mathbf{f}'(D) \, \mathrm{d}A' \tag{12}$$

with $\mathbf{F}'_{\text{Tot}} = \mathbf{F}_{\text{Tot}}/F_0$, and $F_0 = K_{eq} \kappa_0 l_0$. The adhesion area of the circular patch is given by $A'_s = \pi R_s'^2$, where the adhesion radius, R'_s, is found using a scaling law argument of the 'settling phase of the particles' (details in supplementary material, [23])

$$R'_s = \left(\frac{k_B T}{\kappa_0 l_0} \right)^{1/2} \left(\frac{1}{R_1} + \frac{1}{R_2} \right) (R_1 + R_2)^{1/2}. \tag{13}$$

Finally, in a Stokes regime, the aggregation kernel, K_A (in Equation (3a) and (3b)), is proportional to the total force arising from all the bound bonds, $\mathbf{F}_{\text{Tot}}$, and is given by

$$\begin{aligned}
K_A &= \gamma_A F_{\text{Tot}} \\
&= \gamma_A F_0 g' ||\mathbf{f}'(D)|| \pi R_s'^2 \\
&= \frac{4 \kappa_0 l_0^3 k_B T}{A \mu} \, \mathrm{e}^{-r(D'-1)^2} \frac{(R_1 + R_2)^3}{(R_1 R_2)^2} \left(D' - 1 + \frac{1}{\kappa_0 l_0} \left(-2\pi \epsilon_0 \epsilon \psi_1 \psi_2 \frac{2 R_1 R_2}{R_1 + R_2} \frac{\mathrm{e}^{-\kappa D}}{\kappa} \right. \right. \\
&\quad \left. \left. + \frac{A}{6 l_0^2 D'^2} \frac{R_1 R_2}{R_1 + R_2} \right) \right)
\end{aligned} \tag{14}$$

where $\gamma_A = 4 \kappa_0 l_0^3 / A \pi \mu A_{\text{Tot}} K_{\text{eq}}$ is the aggregation contact efficiency parameter and μ is the viscosity of the fluid. Equations (2), (3a), (3b) and 14) along with initial conditions, $b(0, x) = b_0(x)$ (discussed in Section 3.2) constitute the entire system which calculates the size distribution of round floc aggregates. In limit of perfect binding effectiveness (i.e. the fraction of effective binding ligands, $g' \to 1$ and the minimum separation distance, $D' \to 1$) and in a neutral solution with no dissolved ions (i.e. the Debye length, $\kappa^{-1} \to 0$), Equation (14) reduces into the kernel for Brownian diffusion for hard spheres [15],

$$K_A(g' \to 1, \kappa^{-1} \to 0) = K_A^{\text{Br}} = \frac{2 k_B T}{3\mu} \frac{(R_1 + R_2)^2}{R_1 R_2}, \tag{15}$$

which is regularly used for numerous simulations involving purely diffusive kernels [3,19,26]. However, we have used Equation (14) to generate our numerical results in the next section.

To summarize, we have presented a model describing the surface adhesion of round flocs, with the following features:

- Each floc constitutes a rigid spherical core onto which linear, Hookean, spring-like binding ligands are attached and the surface of the coalescing flocs is linked through these ligands. The ligand kinetics is modelled using a differential equation mediated by the bond formation/breakage rates.
- The rigid core of the floc is charged and suspended in an ionic medium. The charge effects are modelled via the repulsive Coulombic interactions and the attractive Van der Waal interactions.

Table 1. Parameters corresponding to the Coulombic interactions, Equation (6) [1].

salt (M)	$\psi_1 (mV)$	ψ_2 (mV)	κ
0.01	−16	−31.7	3.04
0.05	−14	−9.2	1.36
0.5	−10	−3	0.43

3. Numerical results

We assume that the salt dissolved in the fluid is a 1–1 electrolyte. The values of the zeta potentials and the corresponding Debye lengths at different salt concentrations are used from the experiments of Camesano *et al.* which involves adhesion of rigid spherical bacterial surface with silicon nitride atomic force microscopy tip [1]. These values are listed in Table 1. The formula relating the Debye length with the electrolyte concentration is given in [16] (Chapter 14). The viscosity of the fluid (water) at temperature $T = 25°C$, is $\mu = 10^{-3}$ Pa.s. The dielectric constant in vaccum is $\epsilon_0 = 8.854 \times 10^{-12}$, while the permittivity of water at this temperature is $\epsilon = 78.5$. The Hamaker constant measuring the macroscopic Van der Waal sphere–sphere interaction is fixed at 2.44 $k_B T$ [15].

3.1. *Surface potential and bond fraction calculations*

In this section we present the salient features of the DLVO interaction potential, $W(D)$, as well as the evolution of the fraction of bound ligands, g, versus select values of material parameters. Figure 2 highlights the interaction potential versus the minimum separation distance, D, at various salt concentrations (represented by the corresponding Debye length, κ^{-1}).

A weak electrolytic solution (e.g. $\kappa = 3.04$, solid curve, Figure 2(a)) has a large positive potential energy barrier at short separation distances, since a weak salt solution results in diffuse screening length surrounding the charged surfaces which hinders adhesion (also see the corresponding floc-size distribution dynamics in Figure 4(b)). Conversely, for sufficiently concentrated solution (e.g. $\kappa = 0.43$ curve, Figure 2(a)), the energy barrier is reduced and aggregation is favoured. The *primary minima* (shown in Figure 2(a)) is unphysical, since at very short separation distances, non-DLVO interactions are dominant and that prevents the surface of the particles from coming into true contact. The regions of attraction/repulsion of this potential is inferred from surface force per binder, $\mathbf{f}$ (Figure 2(b)). For sufficiently concentrated salt solution these forces are attractive ($\mathbf{f} > 0$ for all D, $\kappa = 0.43$, dotted curve, Figure 2(b)) and hence, adhesion is always favoured. Otherwise at lower salt concentrations, the general feature is that at intermediate distances ($2 \, nm < D < 15 \, nm$), the short range repulsive Coulombic forces are dominant while at longer distances ($D > 15 \, nm$), the adhesive forces are dictated by the attractive spring force of the stretched binders. We choose to conduct our numerical simulations for calculating floc-size distribution at a minimum separation distance $D = 11 \, nm$, a point far away from the *primary minima* where the adhesive forces are attractive.

In stagnant fluid conditions, the bound ligand fraction, $g(D)$, is symmetric about the mean rest length of the binders, l_0 (i.e. g is symmetric about $D = l_0$ or $D' = 1$, Equation (10)). The adhesion mechanism is more efficient for elastic binders (i.e. springs with lower stiffness, κ_0), since these binders have a non-zero attachment over a larger contact area (e.g. compare the non-zero region in Figures 3(a) versus 3(b)). Consequently, we expect the formation of larger aggregates in the size distribution dynamics of flocs with elastic binders, as discussed in the next section.
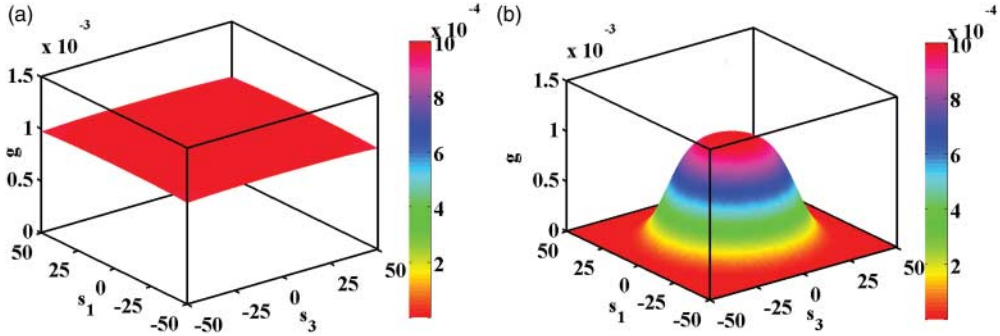
Figure 3. Sticking probability g versus spatial coordinates (s_1, s_3) with spring stiffness (a) $\kappa_0 = 10^{-5}\,\mathrm{Nm}^{-1}$ and (b) $\kappa_0 = 10^{-2}\,\mathrm{Nm}^{-1}$. The radius of the two identically colliding flocs is $R = 1\,\mu\mathrm{m}$. The elastic ligands (or bonds with lower spring stiffness) have a larger contact area (s_1, s_2) with a non-zero collision impact.

Table 2. Parameters common to all simulations [23].

Parameter	Value	Units
κ_0	$(0.01 - 10) \times 10^{-3}$	$\mathrm{N\,m^{-1}}$
l_0	10^{-8}	m
A_{Tot}	10^{9}	–
$K_{\mathrm{on}}^{*}/K_{\mathrm{off}}^{*}$	10^{-12}	–

3.2. *Floc volume distribution*

Next, we describe the floc volume distribution dynamics which uses the ligand-mediated binder kinetics and DLVO interaction potential. We solve the complete population balance model (Equation (2)) using the adhesion kernel described earlier. We employ the discretization scheme developed by Ackleh and Fitzpatrick [4], Banks and Kappel [2] and adopted by Prigent *et al.* [28]. The parameters used in the simulations are listed in Table 2. The convergence of the scheme was tested using standard test functions [7]. A linear relationship between the L^{∞}-error and the mesh-size, δx was found using this first-order approximation scheme. The initial number density is chosen as $b_0(x) = 3.89 \times 10^9\,\mathrm{e}^{-1.56x} + 7.47 \times 10^{-4}\,\mathrm{e}^{-0.00676x}$, where the coefficients are fit to the experimental data from the Younger Lab [7]. The solutions in Figure 4 are shown at time $T = 100\,\mathrm{min}$. We chose 1 femtoliters (fL) as a lower bound $\underline{x}$ in our simulations. Although the
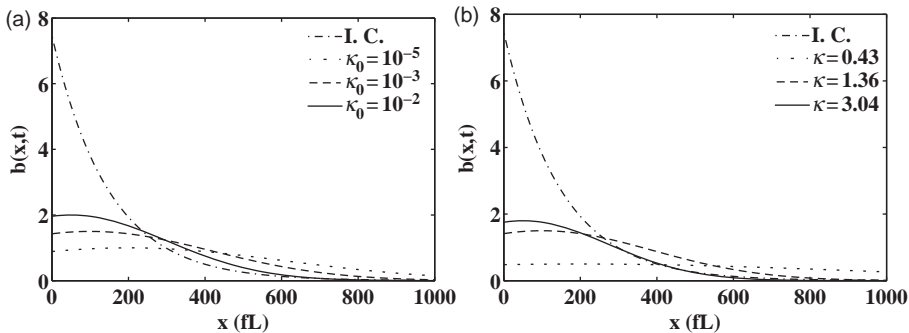
Figure 4. Floc number density distribution, $b(x, t) \times 10^6$, versus floc volume in fL, at time $T = 100\,\mathrm{min}$ for (a) different binder stiffnesses but a fixed screening length, $\kappa = 1.36$, and (b) different screening lengths but a fixed spring stiffness $\kappa_0 = 10^{-3}\,\mathrm{Nm}^{-1}$. The dash-dot curve in these figures is the initial condition, $b_0(x)$.

model allows the upper bound, $\bar{x}$, of the domain to go unrestrained, but the results are presented inside the window $1 \leq x \leq 1000$ fL.

Figure 4 highlights the floc number density for various volume intervals, x, and at different material parameters, κ_0, κ. The studies suggest that stiff binders lead to fewer large aggregates (i.e. $b(x, T, \kappa_0 = 10^{-2}) < b(x, T, \kappa_0 = 10^{-3}) < b(x, T, \kappa_0 = 10^{-5})$ for $x \geq 600$ fL). This is not surprising since aggregation is influenced by the sticking probability, g (Equation (10)). A value of g which is non-zero over a larger contact area (s_1, s_3), implies that the two flocs close to each other are more likely to coalesce leading to bigger flocs (e.g. compare the values of g in Figure 3(a) versus Figure 3(b)). Conversely, for stiff binders, the sticking probability is significant over a smaller region of contact and does not favour formation of large aggregates (Figure 4(a)). Surface adhesion is comparatively stronger in highly ionic fluids (i.e. the curves which are represented by a shorter Debye length, κ, Figure 4(b)). At shorter Debye length, the diffuse charge-shield around the spherical particles become thinner and the particles approach closer to each other, leading to a strong adhesion (Figure 4(b)). In a separate study, we have found that adhesion is favoured in flocs of smaller size (i.e. smaller radius of the spheres). This is effect is explained via a lower DLVO-potential energy barrier in small size particles.

4. Conclusions

We have presented a multi-scale model for the aggregation dynamics of rigid, charged, spherical, micron-sized flocs. This feature is achieved by developing an aggregation kernel which bridges the micro-scale description of ligand initiated binder kinetics and DLVO interactions, with the macro-scale population balance model. The kernel reduces to the well-known Brownian diffusion kernel for hard spheres, in the limit of perfect binding efficiency. The binding kinetics of the flocs is incorporated via the *sticking probability*, a term popularly associated with the floc adhering efficiency, in the colloid literature [19,26]. Numerical predictions about the floc aggregate size at various material and fluid parameters are made. Preliminary investigation in quiescent flow conditions highlight that the adhesion mechanism is favoured if the binding ligands of the flocs are elastic, or the surrounding fluid is highly ionized. The effects of surface deformation which modifies the adhesion area and hence the aggregation kernel [17], spatial inhomogeneities of the material parameters, the non-equilibrium effects, stochasticity and the discrete number of bonds [39] have not been considered in the present study. These effects are the subject of current and future investigations, on the numerical as well as on the experimental front.

References

[1] N.I. Abu-Lail and T.A. Camesano, *Role of ionic strength on the relationship of biopolymer conformation, DLVO contributions, and steric interactions to bioadhesion of Pseudomonas putida KT2442*, Biomacromolecules 4(4) (2003), pp. 1000–1012. doi:10.1021/bm034055f.

[2] A.S. Ackleh and B.G. Fitzpatrick, *Modeling aggregation and growth processes in an algal population model: Analysis and computations*, J. Math. Biol. 35(4) (1997), pp. 480–502. doi:10.1007/s002850050062.

[3] M.U. Bäbler and M. Morbidelli, *Analysis of the aggregation-fragmentation population balance equation with application to coagulation*, J. Colloid Interface Sci. 316(2) (2007), pp. 428–441. doi:10.1016/j.jcis.2007.08.029. http://www.ncbi.nlm.nih.gov/pubmed/17804007

[4] H.T. Banks and F. Kappel, *Transformation semigroups and L1-approximation for size structured population models*, Semigroup Forum 38(1) (1989), pp. 141–155. doi:10.1007/BF02573227.

[5] G. Bell, *Models for the specific adhesion of cells to cells*, Science 200(4342) (1978), pp. 618–627. doi:10.1126/science.347575.

[6] U.S.T. Bihr and A.S. Smith, *Nucleation of ligand-receptor domains in membrane adhesion*, Phys, Rev. Lett. 109(25) (2012), pp. 258101–258105. doi:10.1103/PhysRevLett.109.258101.

[7] D.M. Bortz, T.L. Jackson, K.A. Taylor, A.P. Thompson, and J.G. Younger, *Klebsiella pneumoniae flocculation dynamics*, Bull. Math. Biol. 70(3) (2008), pp. 745–768. doi:10.1007/s11538-007-9277-y.

[8] E.C. Byrne, S.P. Dzul, M.J. Solomon, J.G. Younger, and D.M. Bortz, *Postfragmentation density function for bacterial aggregates in laminar flow*, Phys. Rev. E 83(4) (2011), pp. 41911-1-10. doi:10.1103/PhysRevE.83.041911.

[9] N.G. Cogan and J.P. Keener, *The role of the biofilm matrix in structural development*, Math. Med. Biol. 21(2) (2004), pp. 147–166. doi:10.1093/imammb/21.2.147.

[10] D.F.S. Corezzi and F. Sciortino, *Chemical and physical aggregation of small-functionality particles*, Soft Matter 8 (2012), pp. 11207–11216. doi:10.1039/C2SM26112J.

[11] M. Dembo, D.C. Torney, K. Saxman, and D. Hammer, *The reaction-limited kinetics of membrane-to-surface adhesion and detachment*, Proc. Royal Soc. B 234(1274) (1988), pp. 55–83. doi:10.1098/rspb.1988.0038.

[12] E.A. Evans, *Detailed mechanics of membrane-membrane adhesion and separation. I. Continuum of molecular cross-bridges*, Biophys. J. 48(1) (1985), pp. 175–183. doi:10.1016/S0006-3495(85)83770-X.

[13] B. Gilbert, G. Lu, and C. Kim, *Stable cluster formation in aqueous suspensions of iron oxyhydroxide nanoparticles*, J. Colloid Interface Sci. 313(1) (2007), pp. 152–159. doi:10.1016/j.jcis.2007.04.038.

[14] A. Goldman, R. Cox, and H. Brenner, *Slow viscous motion of a sphere parallel to a plane wall-I Motion through a quiescent fluid*, Chem. Eng. Sci. 22(4) (1967), pp. 637–651. doi:10.1016/0009-2509(67)80047-2.

[15] J. Gregory, *Particles in Water*, CRC Press, Boca Raton, FL, 2006.

[16] J. Israelachvili, *Intermolecular and Surface Forces*, 3rd ed., Academic Press, Amsterdam, 2011.

[17] S. Jadhav, C.D. Eggleton, and K. Konstantopoulos, *Mathematical modeling of cell adhesion in shear flow: Application to targeted drug delivery in inflammation and cancer metastasis*, Curr. Pharm. design 13(15) (2007), pp. 1511–1526. doi:10.2174/138161207780765909.

[18] Z. Jia, C. Gauer, H. Wu, M. Morbidelli, A. Chittofrati, and M. Apostolo, *A generalized model for the stability of polymer colloids*, J. Colloid Interface Sci. 302(1) (2006), pp. 187–202. doi:10.1016/j.jcis.2006.06.011.

[19] A. Jordá, G. Odriozola, F. López, A. Schmitt, and R. Álvarez, *The DLCA-RLCA transition arising in 2D-aggregation: Simulations and mean field theory*, Eur. Phys. J. 5(4) (2001), pp. 471–480. doi:10.1007/s101890170054.

[20] M.R. King and D.A. Hammer, *Multiparticle adhesive dynamics. Interactions between stably rolling cells*, Biophys. J. 81(2) (2001), pp. 799–813. doi:10.1016/S0006-3495(01)75742-6.

[21] C. Korn and U.S. Schwarz, *Efficiency of initiating cell adhesion in hydrodynamic flow*, Phys. Rev. Lett. 97(13) (2006), pp. 138103–138104. doi:10.1103/PhysRevLett.97.138103.

[22] X. Lei, M.B. Lawrence, and C. Dong, *Influence of cell deformation on leukocyte rolling adhesion in shear flow*, J. Biomech. Eng. 121(6) (1999), pp. 636–643. doi:10.1115/1.2800866.

[23] M. Mani, A. Gopinath, and L. Mahadevan, *How things get stuck: Kinetics, elastohydrodynamics, and soft adhesion*, Phys. Rev. Lett. 108(22) (2012), pp. 226104–226105. doi:10.1103/PhysRevLett.108.226104.

[24] B. Marshall, M. Long, J. Piper, T. Yago, and R. McEver, *Direct observation of catch bonds involving cell-adhesion molecules*, Nature 423 (2003), pp. 190–193. doi:10.1038/nature01605.

[25] N.W. Moore and T.L. Kuhl, *The role of flexible tethers in multiple ligand-receptor bond formation between curved surfaces*, Biophys. J. 91(5) (2006), pp. 1675–1681. doi:10.1529/biophysj.105.079871.

[26] G. Odriozola, A. Jordá, A. Schmitt, J. Fernández, R. Garca, and R. Álvarez, *A probabilistic aggregation kernel for the computer-simulated transition from DLCA to RLCA*, Europhys. Lett. 53(6) (2001), pp. 797–803. doi:10.1209/epl/i2001-00210-x.

[27] D. Poland, *The effect of excluded volume on aggregation kinetics*, J. Chem. Phys. 97 (1992), pp. 470–481. doi:10.1063/1.463593.

[28] S. Prigent, A. Ballesta, F. Charles, N. Lenuzza, P. Gabriel, L.M. Tine, H. Rezaei, and M. Doumic, An efficient kinetic model for assemblies of amyloid fibrils and its application to polyglutamine aggregation, PLoS ONE 7(11): e43273 (2012), pp. 1–9. doi:10.1371/journal.pone.0043273.

[29] J.H. Promislow, A.P. Gast, and M. Fermigier, *Aggregation kinetics of paramagnetic colloidal particles*, J. Chem. Phys. 102 (1995), pp. 5492–5498. doi:10.1063/1.469278.

[30] S. Reboux, G. Richardson, and O. Jensen, *Bond tilting and sliding friction in a model of cell adhesion*, Proc. Royal Soc. A 464(2090) (2008), pp. 447–467. doi:10.1098/rspa.2007.0210.

[31] P. Serrano, C. Chin, S. Yiacoumi, and C. Tsouris, *Modeling aggregation of colloidal particles*, Curr. Opin. Colloid Interface Sci. 10(3–4) (2005), pp. 123–132. doi:10.1016/j.cocis.2005.07.003.

[32] S. Sircar and D. Bortz, *Impact of flow on ligand-mediated bacterial flocculation*, Math. Biosci. 245 (2013), pp. 314–321. doi:10.1016/j.mbs.2013.07.018.

[33] M. van Smoluchowski, *Drei Vorträge über Diffusion, Brownsche Bewegung und Koagulation von Kolloidteilchen*, Z. Phys. 17 (1916), pp. 557–571.

[34] P. Somasundaran, V. Runkana, and P. Kapur, *Flocculation and dispersion of colloidal suspensions by polymers and surfactants: Experimental and modeling studies*, in *Coagulation and Flocculation*, 2nd ed., Surfactant Science Series, Vol. 126, H. Stechemesser and B. Dobias, eds., Marcel Dekker, New York, 2005, pp. 767–803.

[35] S. Tabatabaei and T.V.D. Ven, *Tangential electroviscous drag on a sphere surrounded by a thin double layer near a wall for arbitrary particle–wall separations*, J. Fluid Mech. 656 (2010), pp. 360–406. doi:10.1017/S0022112010001199.

[36] W. Thomas, *Catch Bonds in Adhesion*, Annu. Rev. Biomed. Eng. 10 (2008), pp. 39–57. doi:10.1146/annurev.bioeng.10.061807.160427.

[37] A. Zaccone, D. Gentili, H. Wu, and M. Morbidelli, *Shear-induced reaction-limited aggregation kinetics of brownian particles at arbitrary concentrations*, J. Chem. Phys. 132(13) (2010), pp. 134903–134906. doi:10.1063/1.3361665.

[38] J. Zhang and X.Y. Liu, *Effect of protein–protein interactions on protein aggregation kinetics*, J. Chem. Phys. 119 (2003), p. 10972–10976. doi:10.1063/1.1622380.

[39] C. Zhu, *Kinetics and mechanics of cell adhesion*, J. Biomech. 33(1) (2000), pp. 23–33. doi:10.1016/S0021-9290(99)00163-3.